TNO-report
95-CMC-R0614

Torsional vibration analysis of a long propeller shaft system driven by an electric motor (Electric system)

TNO Building and
Construction Research

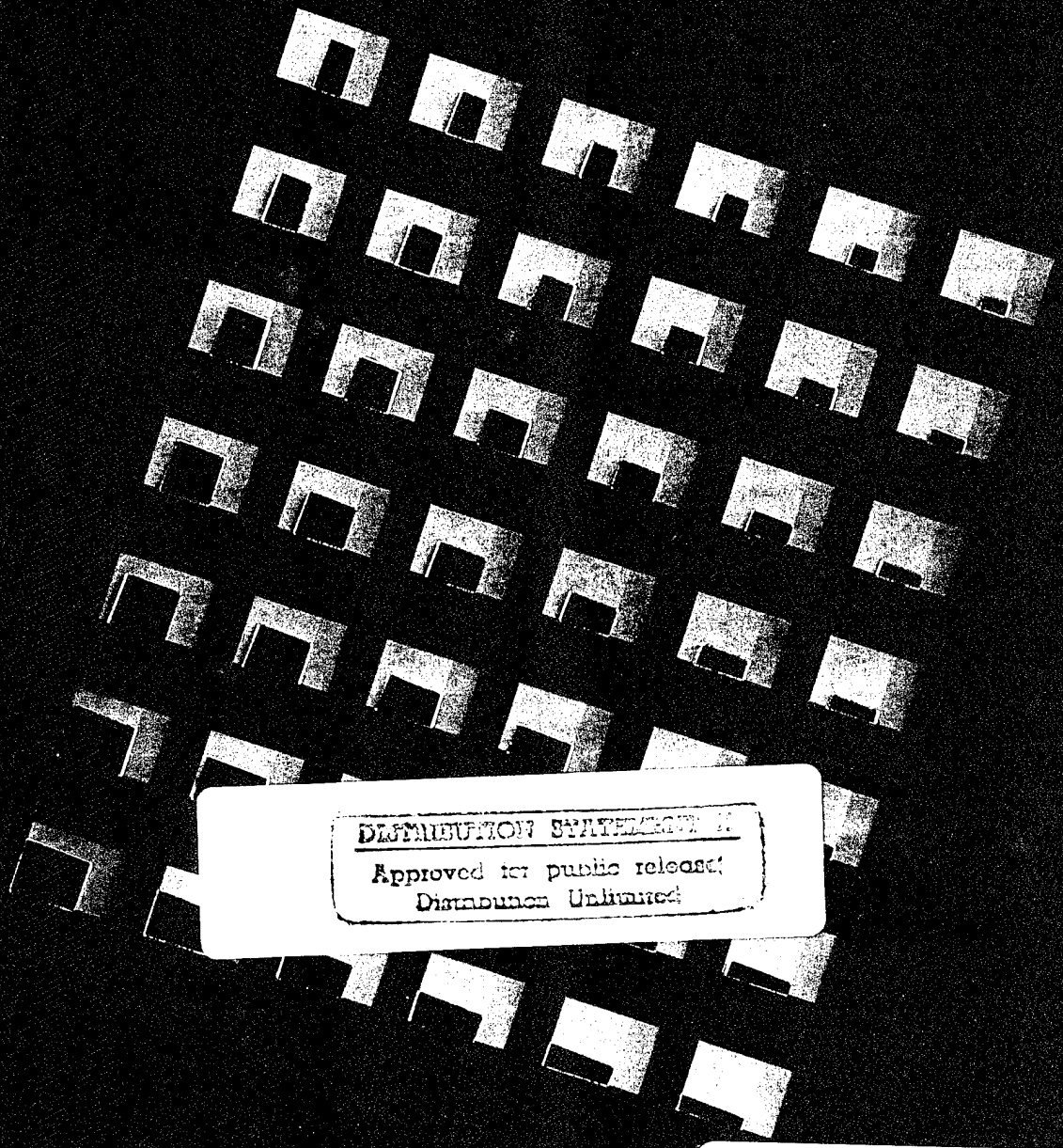

TNO-report
95-CMC-R0614

Torsional vibration analysis of a long propeller shaft system driven by an electric motor (Electric system)

TNO Building and
Construction Research

Lange Kleiweg 5, Rijswijk
P.O. Box 49
2600 AA Delft
The Netherlands

Phone +31 15 284 20 00
Fax +31 15 284 39 90
Telex 38270

Date December 31, 1995

Author(s) ir. H.S.T. Brockhoff
ir. P.P.M. Lemmen

Sponsor : Ministry of Defence
Royal Netherlands Navy
P.O. Box 20702
2500 ES 's-Gravenhage
The Netherlands

Classification
classified by : ir. I.P. Barendregt
Classification date : December 31, 1995

Title : ONGERUBRICEERD
Managementuittreksel : ONGERUBRICEERD
Report text : ONGERUBRICEERD
Appendices : ONGERUBRICEERD

The classification designation ONGERUBRICEERD is equivalent to UNCLASSIFIED.

Contract number : A94/KM/125
Project number : 42775649
Approved : ir. G.J. Meijer
Visa : ir. G.T.M. Janssen

Pages : 51 (incl. appendix, excl. RDP and distribution list)

Managementuittreksel

Titel : Torsional vibration analysis of a long propeller shaft system driven by an electric motor (Electric system)
Auteurs : ir. H.S.T. Brockhoff, ir. P.P.M. Lemmen
Datum : 31 december 1995
Opdrachtnr. : A94/KM/125
IWP-nr. : 792
Rapportnr. : 95-CMC-R0614

Bij het ontwerpen van nieuw te bouwen marineschepen wordt steeds vaker overwogen gebruik te maken van niet-conventionele voortstuwingssystemen. Systemen op basis van een elektrische voortstuwing staan momenteel sterk in de belangstelling. Ook het gebruik van niet-conventionele scheepsvormen kunnen speciale eisen stellen aan het voortstuwingssysteem. Een recent voorbeeld hiervan is het Amfibisch Transport Schip (ATS), waar een keuze werd gemaakt tussen een diesel-directe voortstuwing en een diesel-elektrische. Door de speciale vorm van het ATS zou in beide gevallen gebruik gemaakt moeten worden van een zeer lange schroefas: 74 m voor de diesel-directe voortstuwing en 43 m voor de diesel-elektrische voortstuwing.

Met als doel te onderzoeken of bij gebruik van dergelijke lange schroefassen de gevoeligheid voor torsietrillingen zodanig wordt dat ontoelaatbare torsietrillingsproblemen zullen optreden, zijn een tweetal case studies uitgevoerd naar het torsietrillingsgedrag van beide hiervoor genoemde voortstuwingssystemen. Dit rapport beschrijft de analyse van het elektrische systeem. De analyse van het diesel-directe voortstuwingssysteem is beschreven in TNO rapport 95-CMC-R0615.

Inmiddels is voor het ATS gekozen voor een diesel-elektrische voortstuwing. Deze keuze is niet bepaald door het torsietrillingsgedrag.

De hoofdconclusie van deze studie is dat in het elektrische voortstuwingssysteem geen problemen door torsietrillingen zijn te verwachten. Wel dient aandacht te worden geschonken aan het gedrag van het systeem bij lage toerentallen van de elektromotor. Bij toerentallen van de elektromotor beneden 70 omw./min is er een zeker gevaar is voor het optreden van *gear hammer* in de tandwielkast. Dit betekent dat de tandwielkast zodanig moet worden ontworpen dat deze hiertegen bestand is of dat moet worden voorkomen dat de elektromotor langdurig draait op toerentallen beneden de 70 omw./min.

Uit een vergelijking van het elektrische voortstuwingssysteem met het diesel-directe systeem blijkt dat de torsietrillingen in het elektrische systeem significant lager zijn dan die in het diesel-directe voortstuwingssysteem.

Contents

1 Introduction

In today's designs for naval vessels the use of unconventional propulsion systems is often considered. Propulsion systems based on electric motors and/or combinations with diesel engines or gas turbines may be very attractive from a technical point of view. Also the shape of the ship may be unconventional. A recent example in the Royal Netherlands Navy is the design of the Amphibious Transport Ship (ATS), where a choice will be made between a diesel-direct propulsion system and a diesel-electric system. Owing to the special shape of the ATS in both cases a unusual long propeller shaft will be used: 74 m for the diesel-direct system and 43 m for the diesel-electric system.

In order to investigate whether the use of such long propeller shafts may cause unacceptable sensibility to torsional vibrations, both previous mentioned systems have been analyzed. This report describes the analysis and results for the electric system. The analysis of the diesel-direct system has been described in [R.1].

The torsional vibration analyses have been performed by using the computer program TORPACK [R.2]. The results have been verified according to Lloyd's Register of Shipping [R.5].

Chapter 2 describes the model of the propulsion system.
Chapters 3 to 6 and the accompanying tables and figures show the results of the analyses.
Conclusions are drawn in chapter 7.

Note: in this report all vibratory frequencies will be presented in two units: cycles per second (Hz) and cycles per minute (c/min). The notation in c/min was added for easy comparison of the vibratory frequencies with the rotor speed of the electric motor, which will be presented in revolutions per minute (r/min) only.

2 Model of the electric propulsion system

In this chapter a description is given of the numerical model as used in the torsional vibration analyses. Standard input values such as rotational inertias and stiffnesses are presented in section 2.1. Input values for the electric motor are presented in section 2.2 and for the propeller in section 2.3.
Data has been used which was available at the start of the project, which was early 1994.

2.1 Overall model of one propulsion system

The diesel-electric propulsion system of the Amphibious Transport Vessel as a whole consists of:
- four diesel-generator units;
- two electric propulsion systems, one starboard and one port.

As the diesel-generator units will have no effect on the long propeller shaft, these have not been taken into account in this study. So, this analysis incorporates the proper *propulsion part* of the diesel-electric propulsion system only.

The electric-propulsion systems on starboard and on port are equal, except for the direction of rotation. Therefore it is sufficient to model only one propulsion system.

Figure 2.1 shows the model of the electric propulsion system. The dimensions in this drawing do not correspond with actual values as it is only a schematic representation of the model. Figure 2.2 shows the model of the long propeller shaft more in detail. In these figures masses are referred to as M_i and springs as K_i.
The model contains relevant rotational mass moments of inertia and torsional stiffnesses from:
- the electric motor;
- the flexible coupling;
- the gear transmission;
- the long propeller shaft;
- the propeller.

The long propeller shaft has been modelled with 12 masses (and 11 springs in between). This ensures a sufficient fine segmentation of the shaft to describe the vibratory behaviour accurately.

Table 2.I shows the rotational mass moments of inertia for each mass in the model and table 2.II shows the torsional stiffnesses of the springs.
The data in these tables has been gathered from the documents listed in chapter 8. In this report these documents are referred to by means of indices D.x between square brackets.

The rotational mass moments of inertia J_{Mi} of the masses on the long propeller shaft have been obtained from:

$$J_{Mi} = J_{shi} + J_{compi} \tag{1}$$

where J_{shi} is the contribution to the inertia of the shaft itself and J_{compi} the contribution of components such as liners.

The terms J_{shi} follow from:

$$J_{shi} = (\pi/32) \cdot \rho \cdot l_{Mi} \cdot (d_u^2 - d_i^2)^2 \qquad (2)$$

In this equation l_{Mi} is the length of the structural part represented by mass M_i, ρ is the density of steel, d_u is the shaft outer diameter and d_i is the shaft inner diameter. The terms J_{compi} are evenly distributed inertias of the components.

For the propeller the added mass of the water has been included. This will be described in section 2.3.

The torsional stiffnesses K of the springs of the long propeller shaft follow from:

$$K = G \cdot I_p / l_K = \pi \cdot G \cdot (d_u^2 - d_i^2) / (32 \cdot l_K) \qquad (3)$$

In this equation G is the shear modulus, I_p is the polar area moment of inertia and l_K is the length of the considered spring.

Note: for the massive shafts (springs 1, 3 and 5) equations (2) and (3) have been used with $d_i = 0$.

The last column of table 2.II contains values for equivalent massive diameters. These values are used to determine shear stresses in the response analyses. As the computer program cannot handle hollow shafts, equivalent massive diameters d_{eq} are used for the long propeller shaft. The equivalent massive diameter follows from equating the section factor of a hollow shaft and the section factor of the equivalent massive shaft:

$$d_{eq} = \{ (d_u^4 - d_i^4) / d_u \}^{1/3} \qquad (4)$$

It should be noted that in the computer program the input of the torsional stiffnesses are separated from the input of the shaft diameters. The stiffnesses of the hollow shafts have been calculated previously by using the actual diameters of the hollow shafts, thus d_u and d_i.

According to [D.6] the long propeller shaft is made of steel with a minimum tensile strength of 580 N/mm^2.

The model contains one gear transmission, i_4 in figure 2.1. The speed ratio of this transmission is 4.9524 [D.4, D.5].

Spring number 2 represents the flexible coupling which is a Spiroflex coupling [D.3], type KJ 330.

The internal damping of the shafts has been modelled by means of *complex damping* in the springs. Complex damping is defined as a damping proportional to displacement but in phase with the velocity of a harmonically oscillating system [R.3]. For all springs in the system (except for spring 2 representing the flexible coupling) a complex damping $\delta = 0.004$ has been used. This is a low value (thus conservative) as commonly used when modelling the shafts in torsional vibration analyses.
Note: this complex damping $\delta = 0.004$ is equivalent to a relative damping $\xi = \delta / 2 = 0.002$ (ratio relative to critical damping) in a resonating one-mass-spring-damper system.

The system contains a flexible coupling (spring 2) made by Spiroflex, according to [D3]. The relative damping ψ of this flexible coupling is expressed as the ratio of the dissipated energy per cycle over the peak value of the internal elastic energy in the flexible coupling. According to the manufacturer's specifications [D.3] this relative damping $\psi = 1.5$. This is equivalent to a relative damping $\xi = \psi / (4*\pi) = 0.119$ (ratio relative to critical damping) in a resonating one-mass-spring-damper system.

2.2 Model of the electric motor

Each propeller is driven by an electric motor. The main motor characteristics are:

Type	: asynchronous induction motor
Nominal power	: 7500 kW
Nominal rotor speed	: 906 r/min
Supply frequency at nominal rotor speed	: 60.4 Hz (4 times rotor speed)

The static damping coefficient b_m of the electric motor has been determined using the gradient of the torque versus rotor speed characteristic. This has been described in appendix A. It is assumed that the ratio of voltage over frequency arranged by the controller is constant. Then it follows that b_m does not depend on the rotor speed. Using the derivation of appendix A it was found that the motor can be modelled by a viscous damper with a damping value $b_m = 1.66*10^4$ N.m.s/rad. Because of uncertainties of the previous assumption this value for b_m could be different in a real system. Therefore it was decided to perform sensitivity analyses. In these analyses the influences of variations in b_m on the obtained results are investigated. These are described in chapter 6.

Note
During the preparation of this report, it appeared that a calculation error had been made in appendix A: the value of the viscous damper should be $b_m = 1.66*10^5$ N.m.s/rad (corrected now in appendix A) instead of the value of $1.66*10^4$ N.m.s/rad as found earlier and used as a basis for the calculations in this report.
In order to judge the effect of this error of a factor 10 in damping, a part of the sensitivity analyses as described in chapter 6 have been extended with this higher damping value. As expected, the higher motor damping will lead to lower vibratory torques and stresses. Thus, the calculations presented in this report are 'at the safe side'.

Information on the harmonics of the electric motor are specified in [D.2]. Amplitudes of the excitation torques are given for supply frequencies ranging from 1 to 64 Hz. As the motor has 4 poles, this corresponds to rotor speeds ranging from 15 to 960 r/min. In [D.2] excitation torques amplitudes are specified as a percentage of the 'nominal torque'. However, the meaning of 'nominal torque' was not clear from the manufacturer's information: either it means 'actual mean torque at a certain rotor speed' or it means 'mean torque at the nominal rotor speed', which is 906 r/min. In consultation with the Royal Netherlands Navy it was decided to use the most severe interpretation, i.e. torque reference = mean torque at 906 r/min.

2.3 Model of the propeller

Following data were available for the propellers of the ATS with the electric propulsion system [D.8]:

Propeller type	: 5 blades, fixed pitch
Number of propellers	: 2
Diameter	: 4 m
Mean propeller pitch ratio $P / D_{0.7}$	: 1.16
Blade area ratio	: 0.72

Torque versus speed
A quadratic relationship has been assumed for the mean propeller torque versus propeller speed. As power is equal to torque times speed, this means a third power relationship for propeller power versus propeller speed. The propeller torque has been based on the following data:

Nominal propeller power	: equal to the electric motor = 7500 kW
Nominal propeller speed	: (nominal rotor speed / gear transmission) = 906 / 4.9524 = 182.9 r/min

Note: the propeller power is taken equal to the power of the electric motor. Thus, no energy losses in the gearing system and in the long propeller shaft have been taken into account. This means that in a real system the mean propeller torque will be about 5 % lower.

Added mass and damping
Added mass and damping coefficients for the propeller have been obtained by interpolation from the tables given in [R.7]. These coefficients describe the hydrodynamic reaction forces that act on the propeller which is vibrating at the blade frequency. The values tabulated in [R.7] follow from analyses of the Wageningen B4 screw types with zero rake. These analyses were based on the unsteady lifting surface theory. The required input for interpolation from the tables are the propeller diameter, the blade area ratio and the pitch ratio.
Using these values it follows from the tables in [R.7] that the added mass of the propeller is 2283 kg.m^2. Together with the mass moment of inertia of the propeller itself the total inertia of the propeller becomes 2283 + 5310 = 7593 kg.m^2.
The dimensional damping coefficient b_p of the damping torque acting on the propeller depends on the rotational frequency of the propeller Ω_p. Using the tables in [R.7] it follows that:

$$b_p = 3647\ \Omega_p \qquad \text{[N.m.s/rad]}$$

where Ω_p is in rad/s.

Blade order excitations
Due to the presence of a wake, the propeller operates in a circumferentially varying flow field. This results in non-constant hydrodynamic torques [R.6]. The resulting torque is supposed to be the summation of a constant part (the mean propeller torque) and two harmonic parts of 1st and 2nd blade order frequency. The 1st blade order frequency is the number of blades times the rotational frequency of the shaft. The 2nd blade order frequency is twice the 1st blade order frequency.
The amplitude of the 1st blade order excitation torque is assumed to be 3 % of the mean propeller torque. This value is taken equal to the value used in [R.8] as dimensions of both propellers are almost equal. The amplitude of the 2nd blade order excitation torque is assumed to be 1.5 % of the mean propeller torque.

3 Natural frequencies and mode shapes

Table 3.I shows the natural frequencies of the system calculated by the computer program TORPACK [R.2]. The corresponding mode shapes are shown in figures 3.1 to 3.15.

From these figures it can be seen that the gradient of the modal rotation is relatively large at the flexible coupling (spring 2). This was to be expected as the stiffness of this component is relatively low.

With respect to the discrete dampers and excitation torques acting on both the rotor (mass 1) and the propeller (mass 17) it can be seen that the rotations of the these masses are relatively small for modes 2 up to 15. This is an important feature as the energy going with these excitation torques and damping torques is directly proportional to the modal rotations of these masses.

4 Critical rotor speeds

If one of the harmonics of an excitation torque coincides with one of the natural frequencies of the system the amplitude of vibration may become large. The rotor speeds at which such resonance may occur are called the critical rotor speeds c_s. If the excitation torque acts on a mass with the same rotational speed as the rotor then c_s follows from [R.4]:

$$c_s = f_i / n \tag{5}$$

in which f_i is the natural frequency of mode i and n is the order of the excitation torque.
If the system contains one or more gear transmissions between the rotor and the mass with the excitation torque then the critical rotor speed c_s follows from:

$$c_s = f_i * i / n \tag{6}$$

in which i is the speed ratio between the rotor and the considered mass and n is the order of the excitation torque acting on that particular mass.

Table 4.I to 4.III show the critical rotor speeds for relevant harmonics of the propeller and the electric motor. It is noted that these results do not contain any information on the amplitude of vibration. They just represent those rotor speeds for which a resonance increase of the system might occur. Therefore, in response analyses special attention must be paid to these speeds.

5 Forced vibration response

5.1 Results for the shafts

Table 5.I shows results for the maxima of vibratory torques and stresses in the shafts together with the rotor speeds (inadvertently in the figures called *engine* speed) for which these maxima occur. The allowable vibratory stresses according to Lloyd's Register of Shipping [R.5] and the vibratory stresses as percentages of the allowable stresses are shown in the last two columns of this table. It is noticed that specified values for the allowable stresses are for continuous running at the nominal rotor speed (906 r/min). For rotor speeds different from the nominal motor speed, higher stresses are allowed, similar to the dashed line shown in fig. 5.2.

For the determination of the allowable stresses in the long propeller shaft, the following has been taken into account:

- springs 1 and 3 to 9 are classified as 'intermediate shafts', thus according to section 2.6 of Lloyd's Register of Shipping [R.5];
- for springs 6 to 9 a factor of 0.75 has been applied, because of 'loose couplings' according to section 2.6.1 of Lloyd's Register of Shipping [R.5];
- springs 10 to 16 are classified as 'screwshafts', thus according to section 2.5 of Lloyd's Register of Shipping [R.5];
- for all shafts a material factor k_m= 1.321 according to section 2.8.1 of Lloyd's Register of Shipping [R.5] has been applied to account for the minimum tensile strength of 580 N/mm^2 of the shaft's steel.

From table 5.I it follows that the highest loaded spring is the shaft of the electric motor (spring 1) for which the vibratory stress reaches 28 % of the allowable stress. This maximum occurs at a rotor speed of is 795 r/min. Figure 5.1 shows the calculated vibratory stress in the shaft of the electric motor as a function of the rotor speed. Figure 5.2 shows this same stress (at a different scale), together with the allowable stress. Also shown in figure 5.1 is the second most critical part of the system (spring 6), which is part of the long propeller shaft.

It can be seen from table 5.I and figures 5.1 and 5.2 that for the entire range of relevant rotor speeds all vibratory stresses are far less than the allowable values.

Table 5.II shows the contribution of each harmonic to the response of the shaft of the electric motor (spring 1) at a rotor speed of 795 r/min. From these results it can be seen that the resonant rise at this rotor speed is caused by the harmonic of the 6th order of the electric motor. The excitation frequency of this harmonic coincides with the natural frequency of mode 5 (see table 4.I, sixth column, sixth row). At this mode shape only the flange connection between the electric motor and the flexible coupling shows a large amplitude, see figure 3.5.

Table 5.III shows the contribution of each excitation torque to the response of the highest loaded part of the long propeller shaft (spring 6) for a rotor speed of 30 r/min. This is the critical rotor speed for this spring as can be seen from figure 5.1. Again the resonance rise is caused by the 6th order harmonic of the electric motor. In this case the harmonic coincides with the natural frequency of mode 1 (see table 4.I, second column, sixth row).

5.2 Results for the flexible coupling

Table 5.IV shows calculated maxima for the vibratory torque and the dissipated power in the flexible coupling (spring 2). Allowable values as supplied by the manufacturer [D.3] are shown in the third column. Similar to the shafts, the vibratory torques are small and far less than the allowable values as specified by the coupling manufacturer.

5.3 Results for the gear transmission

Figure 5.3 shows the vibratory torque in the gear transmission together with the mean torque (static transmission torque). Fig. 5.4 shows the same results in a different way: the vibratory torque is shown as a percentage of the mean torque.

Lloyd's Register of Shipping [R.5] recommends that the vibratory torque in a gear transmission should not, in general, exceed one-third of the full transmission torque at critical rotor speeds near the maximum rotor speed. From figures 5.3 and 5.4 it can be seen that this requirement has been fulfilled.

For rotor speeds different from speeds near the maximum rotor speed there are no requirements or recommendations regarding gear transmissions in Lloyd's Register of Shipping [R.5]. In practice it is recommended that for these rotor speeds (i.c. rotor speeds different from speeds near the maximum rotor speed), the vibratory torque should not exceed 70 % of the mean torque. From figures 5.3 and 5.4 it can be seen that for rotor speeds above 70 r/min this requirement has been fulfilled. For lower rotor speeds this is not the case.
This means a certain danger for so-called *gear hammer* at rotor speeds below 70 c/min. Therefore, provisions must be taken that the gear box has been designed for this situation or that no continuous running will occur for rotor speeds below 70 r/min.
The investigated large ratio of vibratory torque over mean torque in the gear transmission for rotor speeds below 70 c/min is due to the relatively large amplitudes of the harmonics of the electric motor at lower rotor speeds according to [D.2]. It should be noted that this is based on the interpretation of 'nominal torque' as described at the end of section 2.2.

6 Sensitivity analysis

In section 2.2 it has been noted that some uncertainty exists concerning the derived damping coefficient of the electric motor. Therefore it was considered of importance to investigate the sensitivity of the calculated response with respect to the applied damping coefficient b_m of the electric motor.
In addition to the calculations presented in the previous chapters, two calculations have been performed in which b_m was reduced to zero respectively increased by a factor two. The results of these analyses are presented in this chapter.

6.1 Results for the shafts

Table 6.I shows the maxima of vibratory stresses for the observed values of the damping coefficient b_m. Figure 6.1 shows the vibratory stress in the shaft of the electric motor (spring 1) and figure 6.2 shows the same results together with the allowable stress according to Lloyd's Register of Shipping [R.5].
From these results it follows that the vibratory stresses increase if damping of the electric motor is fully omitted, as to be expected. However, the obtained stresses remain small when compared to the allowable stresses. For this situation without damping, the shaft of the electric motor (spring 1) is again the most critical one, with a vibratory stress of 16.3 N/mm^2, which is 60 % percent of the allowable stress (table 5.I) of 27.2 N/mm^2.
If b_m is increased from $b_m = 1.66*10^4$ N.m.s/rad up to $b_m = 3.32*10^4$ N.m.s/rad (thus a factor two), then the vibratory stresses reduce, as expected.

Note
As already described in section 2.2, during the preparation of the report it appeared that the calculations in this report have been based on a damping value $b_m = 1.66*10^4$ N.m.s/rad, whereas this value should be 10 times larger, thus $b_m = 1.66*10^5$ N.m.s/rad.
In order to judge the effect of this error of a factor 10 in damping, the sensitivity analyses have been extended with a new calculation, using this higher damping value. The results for the stresses in the shafts are shown in table 6.I, utmost right column. As expected, the higher damping will lead to lower vibratory torques and stresses. Thus, the calculations in this report are 'at the safe side'.
Note: the results for this higher damping value will lead to lower curves in figures 6.1 up to 6.3. For practical reasons, these figures have not been extended with the curves for this higher damping value.

6.2 Results for the flexible coupling

Table 6.II shows calculated maxima for the vibratory torque and the dissipated power in the flexible coupling (spring 2) in case damping of the electric motor is fully omitted ($b_m = 0$ N.m.s/rad). Allowable values as supplied by the manufacturer [D.3] are shown in the third column. For the flexible coupling it is also found that the vibratory torque increases if damping of the electric motor is fully omitted. The obtained values for the vibratory torque and the dissipated power however are still small and far less than the specified allowable values.

6.3 Results for the gear transmission

Figure 6.3 shows the vibratory torque in the gear transmission as a percentage of the mean torque for the applied values of the damping coefficient b_m. From this figure it can be seen that the torque ratio is almost unaffected by b_m, except for rotor speeds around 200 r/min. For those rotor speeds the torque ratio increases from 10 % up to 20 % if the damping of the electric motor is fully omitted. The value of 20 %, however, is still sufficiently small (see section 5.3).

7 Conclusions

7.1 From torsional vibration analyses on the electric propulsion system of the Amphibious Transport Ship (ATS) it appears that vibratory stresses in this system are low. For the entire range of relevant rotor speeds the vibratory stresses remain far below the allowable stresses specified by Lloyd's Register of Shipping [R.5].

7.2 An uncertainty exists about the meaning of 'mean torque' as specified by the manufacturer of the electric motor [D.2]. In these analyses the most severe interpretation has been used.

7.3 In the flexible coupling values for the maximum torque, the vibratory torques and the dissipated power remain far below allowable values specified by the coupling manufacturer [D.3].

7.4 For rotor speeds below 70 r/min there is a certain danger for so-called *gear hammer.* Therefore, provisions must be taken that the gear box has been designed for this situation or that no continuous running will occur for rotor speeds below 70 r/min.

7.5 A noticeable phenomenon resulting from the great length of the propeller shaft is that, except for the lowest modes, relatively large vibratory rotations occur locally in the propeller shaft whereas rotational vibrations of the rotor and the propeller are small. As the discrete dampers in the system act on these two masses only, local vibrations in the long propeller shaft are almost solely controlled by internal damping of the shaft. However, stresses resulting from these relatively large vibrations, are low.

7.6 From a comparison of the electric system with the diesel-direct system [R.1] it is concluded that torsional vibrations in the electric system are significantly lower than those in the diesel-direct system: 1/3 to 1/5 for the vibratory stresses in the long propeller shaft, 1/10 for the vibratory torques in the flexible coupling and 1/20 for the vibratory torques in the gear transmission.
Note: this conclusion has been drawn up in chapter 7 of the report on the diesel-direct system [R.1].

8 References

General references

[R.1] Brockhoff, H.S.T. and Lemmen, P.P.M.
Torsional vibration analysis of a long propeller shaft system driven by two diesel engines
TNO report 95-CMC-R0615, 1995

[R.2] Brockhoff, H.S.T.
TORPACK user's manual
TNO report B-91-0493 (in Dutch), 1991

[R.3] Craigh, R.R.
Structural dynamics - An introduction to computer methods
John Wiley & Sons, 1981

[R.4] Den Hartog, J.P.
Mechanical Vibrations
4th edition
McGraw-Hill Book Company, 1956

[R.5] Lloyd's Register of Shipping
Rules and Regulations for the Classification of Ships
Part 5: Main and Auxiliary Machinery
Chapter 2: Oil engines
Chapter 6: Shaft Vibration and Alignment
Lloyd's Register of Shipping, January 1994

[R.6] Blevins, R.D.
Flow-induced vibration
Van Nostrand Reinhold, 1990

[R.7] Hylarides, S. and Gent, W. van
Hydrodynamic reactions to propeller vibrations
Trans I Mar E (C) Vol. 91, Conference No. 4, Paper C37

[R.8] Bos, J. and Brockhoff, H.S.T.
Torsional and bending propeller shaft vibrations of a GM-frigate
TNO report B-91-0992, 1991

Documentation concerning the electric motor

[D.1] Blokland, A.J.
Berekeningen TNO t.b.v. elektrische voortstuwing
Koninklijke marine, DMKM/PFS, 12 oktober 1993 (handwritten, in Dutch)

[D.2] *Torque spectrum electric motor 60.4 Hz, 7500 kW, 3300 V*

Documentation concerning the flexible coupling and the gear transmission

[D.3] *Highly Elastic Shaft Coupling Spiroflex KJ*
Mannesmann Rexroth, RDE 75411 02,89

[D.4] *Torsion Vibration Scheme, Red. Gear GCH 900*
Mannesmann Rexroth, Drwg. no. 4/4727/5022/0, 18-10-1993

[D.5] *Navilus GC - Marine Reduction Gear*
Mannesmann Rexroth, RDE 75200 12.88

Documentation concerning the long propeller shaft

[D.6] *ATS diesel electric version - Shaftline dimension report*
NEVESBU document no. 2400.11, 27th September 1993

[D.7] *Diesel electric version - Report on shafting vibration calculation (whirling)*
NEVESBU document no. 2400.81, 4th October 1993

Documentation concerning the propeller

[D.8] *ATS diesel electric - Powering estimation report*
BAZAN/NEVESBU, NEVESBU document no. 0514.11, 26th August 1993

Tables

Description	Mass number	Inertia [kg.m^2]
Rotor	1	540.00
Outer part flexible coupling	2	142.40
Inner part flex. coupling + input shaft gear transmission	3	63.30
Input pinion gear transmission	4	8.65
Output wheel gear transmission	5	1388.00
Output shaft gear transm. + M_1 shaft	6	86.12
M_2 shaft	7	19.94
M_3 shaft	8	19.94
M_4 shaft	9	50.68
M_5 shaft	10	89.84
M_6 shaft	11	65.52
M_7 shaft	12	65.52
M_8 shaft	13	65.52
M_9 shaft	14	65.62
M_{10} shaft	15	65.52
M_{11} shaft	16	67.21
Propeller + added mass + M_{12} shaft	17	7618.95

Table 2.I Rotational mass moments of inertia used in the analyses

Spring number	Connected masses	Stiffness [N.m/rad]	Diameter [mm]	Equivalent diameter [mm]
1	1 - 2	$27.60*10^6$	250	-
2	2 - 3	$0.512*10^6$	-	-
3	3 - 4	$54.68*10^6$	265	-
5	5 - 6	$295.60*10^6$	320	-
6	6 - 7	$20.43*10^6$	315/125 [1)]	312.4
7	7 - 8	$20.43*10^6$	315/125 [1)]	312.4
8	8 - 9	$20.43*10^6$	315/125 [1)]	312.4
9	9 - 10	$35.88*10^6$	350/125 [1)]	348.0
10	10 - 11	$37.35*10^6$	380/150 [1)]	376.8
11	11 - 12	$37.35*10^6$	380/150 [1)]	376.8
12	12 - 13	$37.35*10^6$	380/150 [1)]	376.8
13	13 - 14	$37.35*10^6$	380/150 [1)]	376.8
14	14 - 15	$37.35*10^6$	380/150 [1)]	376.8
15	15 - 16	$37.35*10^6$	380/150 [1)]	376.8
16	16 - 17	$119.80*10^6$	410/150 [1)]	407.6

[1)] Hollow shaft

Table 2.II Input of torsional springs

Mode	Frequency [Hz]	Frequency [c/min]	Mode	Frequency [Hz]	Frequency [c/min]
1	3.3	198	9	196.1	11767
2	11.6	694	10	205.3	12317
3	33.1	1984	11	212.9	12772
4	74.0	4441	12	231.7	13903
5	79.2	4754	13	257.3	15435
6	116.3	6976	14	279.6	16774
7	145.1	8706	15	320.8	19247
8	171.6	10298			

Table 3.I Natural frequencies

Mode ---------->	1	2	3	4	5
Nat. freq. [Hz]	3.3	11.6	33.1	74.0	79.2
Nat. freq. [c/min]	198	694	1984	4441	4754
Prop. 1st blade	196	687	1965	4399	4709
Prop. 2nd blade	98	344	983	2199	2354
Rotor order 6	33	116	331	740	792
Rotor order 12	17	58	165	370	396
Rotor order 18	11	39	110	247	264
Rotor order 24	8	29	83	185	198
Rotor order 30	7	23	66	148	158
Rotor order 36	6	19	55	123	132
Rotor order 42	5	17	47	106	113
Rotor order 48	4	14	41	93	99
Rotor order 54	4	13	37	82	88
Rotor order 60	3	12	33	74	79
Rotor order 66	3	11	30	67	72
Rotor order 72	3	10	28	62	66
Rotor order 78	3	9	25	57	61
Rotor order 84	2	8	24	53	57
Rotor order 90	2	8	22	49	53
Rotor order 96	2	7	21	46	50

Table 4.I Critical rotor speeds in r/min for modes 1 to 5

Mode ---------->	6	7	8	9	10
Nat. freq. [Hz]	116.3	145.1	171.6	196.1	205.3
Frequency [c/min]	6976	8706	10298	11767	12317
Prop. 1st blade	6910	8623	10200	11655	12200
Prop. 2nd blade	3455	4312	5100	5827	6100
Rotor order 6	1163	1451	1716	1961	2053
Rotor order 12	581	726	858	981	1026
Rotor order 18	388	484	572	654	684
Rotor order 24	291	363	429	490	513
Rotor order 30	233	290	343	392	411
Rotor order 36	194	242	286	327	342
Rotor order 42	166	207	245	280	293
Rotor order 48	145	181	215	245	257
Rotor order 54	129	161	191	218	228
Rotor order 60	116	145	172	196	205
Rotor order 66	106	132	156	178	187
Rotor order 72	97	121	143	163	171
Rotor order 78	89	112	132	151	158
Rotor order 84	83	104	123	140	147
Rotor order 90	78	97	114	131	137
Rotor order 96	73	91	107	123	128

Table 4.II Critical rotor speeds in r/min for modes 6 to 10

Mode ---------->	11	12	13	14	15
Nat. freq. [Hz]	212.9	231.7	257.3	279.6	320.8
Nat. freq. [c/min]	12772	13903	15435	16774	19247
Prop. 1st blade	12650	13771	15288	16614	19064
Prop. 2nd blade	6325	6885	7644	8307	9532
Rotor order 6	2129	2317	2573	2796	3208
Rotor order 12	1064	1159	1286	1398	1604
Rotor order 18	710	772	858	932	1069
Rotor order 24	532	579	643	699	802
Rotor order 30	426	463	515	559	642
Rotor order 36	355	386	429	466	535
Rotor order 42	304	331	368	399	458
Rotor order 48	266	290	322	349	401
Rotor order 54	237	257	286	311	356
Rotor order 60	213	232	257	280	321
Rotor order 66	194	211	234	254	292
Rotor order 72	177	193	214	233	267
Rotor order 78	164	178	198	215	247
Rotor order 84	152	166	184	200	229
Rotor order 90	142	154	172	186	214
Rotor order 96	133	145	161	175	200

Table 4.III Critical rotor speeds in r/min for modes 11 to 15

Spring number	Rotor speed [r/min]	Vibratory torque [N.m]	Vibratory stress [N/mm^2]	Allowable [1)] stress [N/mm^2]	Percentage of allowable stress [%]
1	795	23400	7.6	27.2	28.0
2	30	2640	-	-	-
3	30	2400	0.7	27.1	2.4
5	30	11600	1.8	26.4	6.8
6	30	11600	1.9	19.8	9.8
7	30	11600	1.9	19.8	9.8
8	30	11600	1.9	19.8	9.8
9	30	11600	1.4	19.5	7.2
10	30	11500	1.1	17.9	6.1
11	30	11500	1.1	17.9	6.1
12	30	11500	1.1	17.9	6.1
13	30	11500	1.1	17.9	6.1
14	30	11400	1.1	17.9	6.0
15	30	11400	1.1	17.9	6.0
16	30	11300	0.8	17.4	4.9

[1)] Allowable stresses for continuous running at nominal rotor speed of 906 r/min

Table 5.I Maxima of vibratory torques and stresses

Excitation source	Vibratory torque [N.m]	Percentage of total [%]
Prop. 1st blade	185.0	0.8
Prop. 2nd blade	7.3	0.0
Rotor order 6	23100.0	98.7
Rotor order 12	81.4	0.3
Rotor order 18	14.8	0.1
Rotor order 24	12.9	0.1
Rotor order 30	13.0	0.1
Rotor order 36	3.5	0.0
Rotor order 42	0.2	0.0
Rotor order 48	0.5	0.0
Rotor order 54	0.4	0.0
Rotor order 60	0.7	0.0
Rotor order 66	0.1	0.0
Rotor order 72	0.2	0.0
Rotor order 78	0.0	0.0
Rotor order 84	0.1	0.0
Rotor order 90	0.0	0.0
Rotor order 96	0.0	0.0
Total	23400.0	100.0

Table 5.II Contribution of each excitation for the shaft of the electric motor (spring 1) at 795 r/min

Excitation source	Vibratory torque [N.m]	Percentage of total [%]
Prop. 1st blade	13.1	0.1
Prop. 2nd blade	7.0	0.1
Rotor order 6	10900.0	94.0
Rotor order 12	81.5	0.7
Rotor order 18	407.0	3.5
Rotor order 24	27.6	0.2
Rotor order 30	47.5	0.4
Rotor order 36	0.9	0.0
Rotor order 42	2.0	0.0
Rotor order 48	0.1	0.0
Rotor order 54	2.5	0.0
Rotor order 60	0.4	0.0
Rotor order 66	111.0	1.0
Rotor order 72	0.6	0.0
Rotor order 78	1.0	0.0
Rotor order 84	0.2	0.0
Rotor order 90	0.3	0.0
Rotor order 96	0.1	0.0
Total	11600.0	100.0

Table 5.III Contribution of each excitation for the highest loaded part of the long propeller shaft (spring 6) at 30 r/min

Quantity	Calculated maximum	Allowable value	Rotor speed at which maximum occurs [r/min]
Maximum torque [kN.m]	79.05	254.0	960
Vibratory torque [kN.m]	2.64	21.3	30
Dissipated power [kW]	0.021	1.48	30

Table 5.IV Results for the flexible coupling (spring 2)

	Damping b_m = 0.0 N.m.s/rad	Damping b_m = $1.66*10^4$ N.m.s/rad	Damping b_m = $3.32*10^4$ N.m.s/rad	Damping b_m = $1.66*10^5$ N.m.s/rad
Spring number	σ_{vib} [N/mm^2]	σ_{vib} [N/mm^2]	σ_{vib} [N/mm^2]	σ_{vib} [N/mm^2]
1	16.3	7.6	4.8	2.3
3	1.1	0.7	0.5	0.1
5	0.4	1.8	0.2	0.4
6	3.2	1.9	1.3	0.5
7	3.2	1.9	1.3	0.5
8	3.2	1.9	1.3	0.4
9	2.3	1.4	1.0	0.3
10	1.8	1.1	0.7	0.2
11	1.8	1.1	0.8	0.2
12	1.8	1.1	0.8	0.2
13	1.8	1.1	0.8	0.3
14	1.8	1.1	0.8	0.3
15	1.8	0.8	0.7	0.3
16	0.8	1.4	0.6	0.3

Table 6.I Results of sensitivity analyses

Quantity	Calculated maximum	Allowable value	Rotor speed at which calculated maximum occurs [r/min]
Maximum torque [kN.m]	79.05	254.0	960
Vibratory torque [kN.m]	4.21	21.3	30
Dissipated power [kW]	0.064	1.48	795

Table 6.II Results for the flexible coupling (spring 2) for damping b_m = 0 N.m.s/rad

Figures

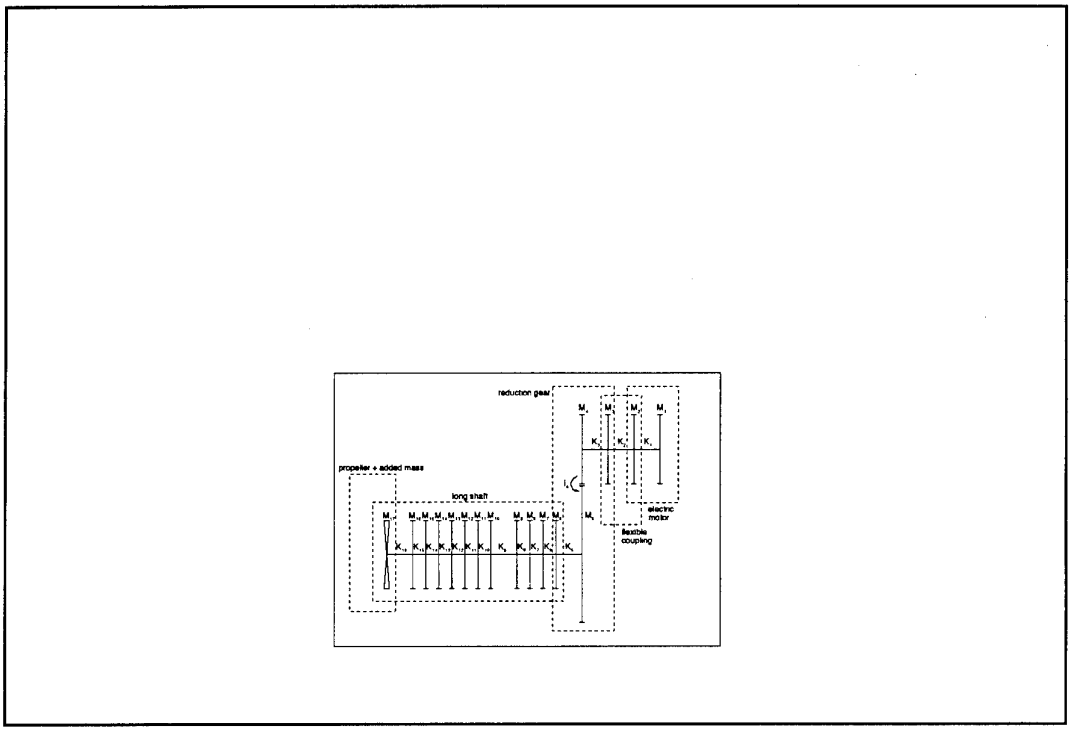

Figure 2.1 Schematic drawing of the model used in the torsional vibration analyses of the electric propulsion system

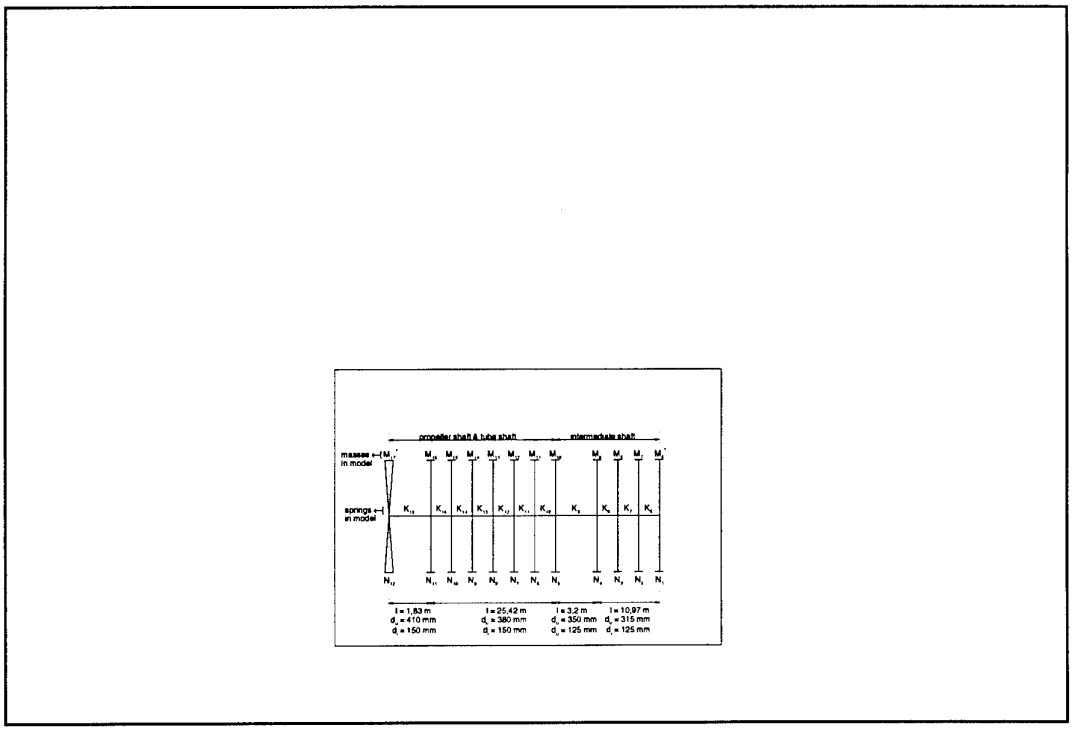

Figure 2.2 Model of the long propeller shaft

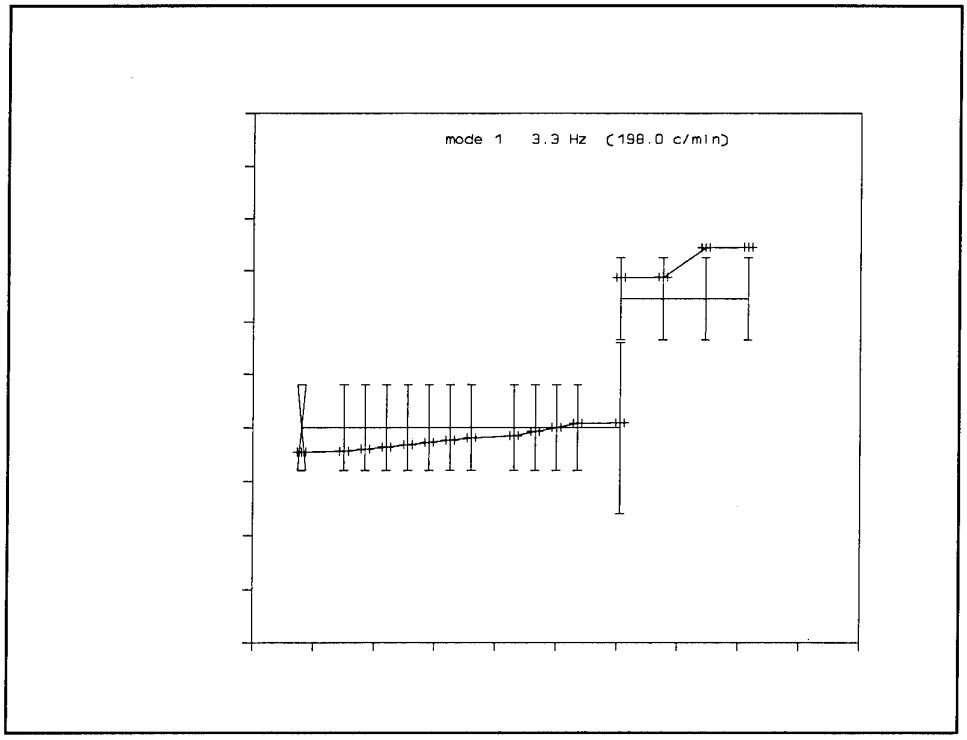

Figure 3.1 Mode 1

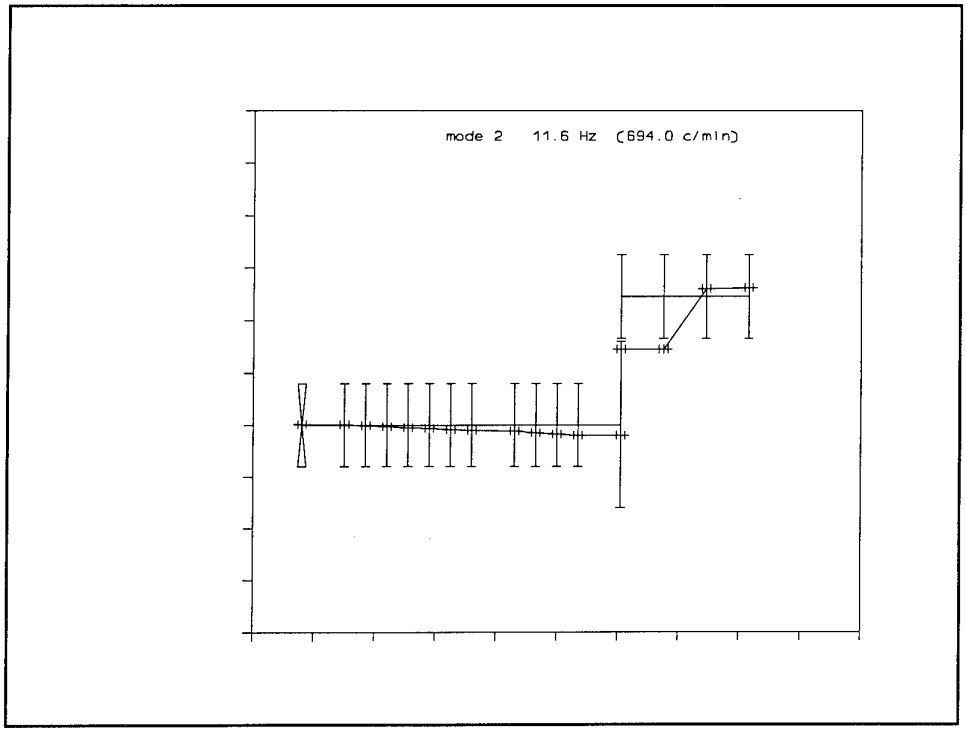

Figure 3.2 Mode 2

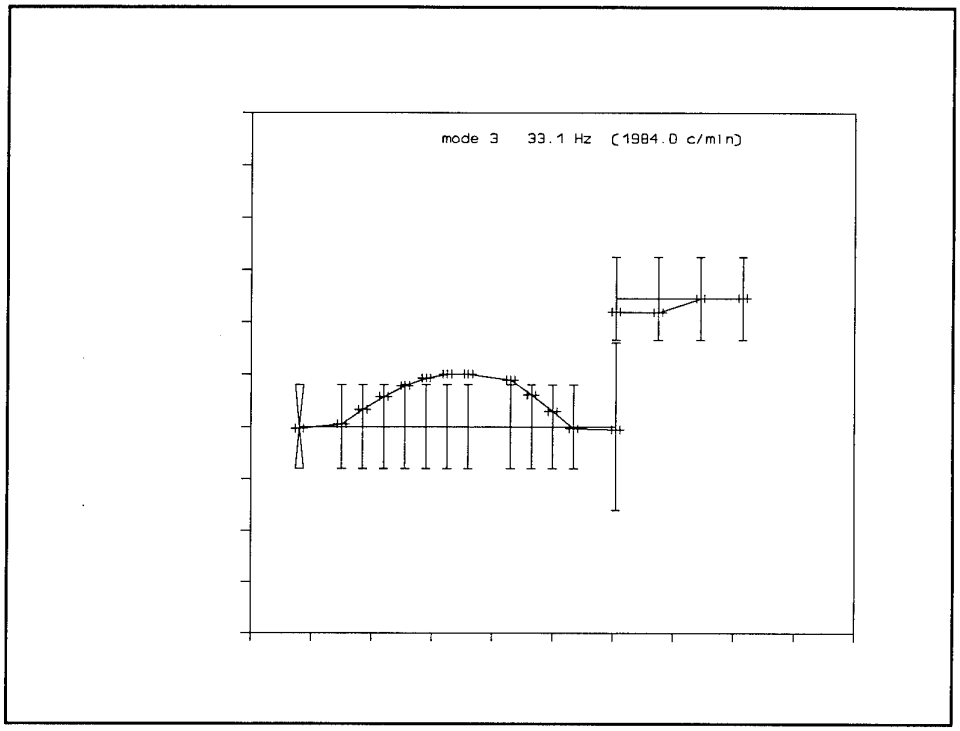

Figure 3.3 Mode 3

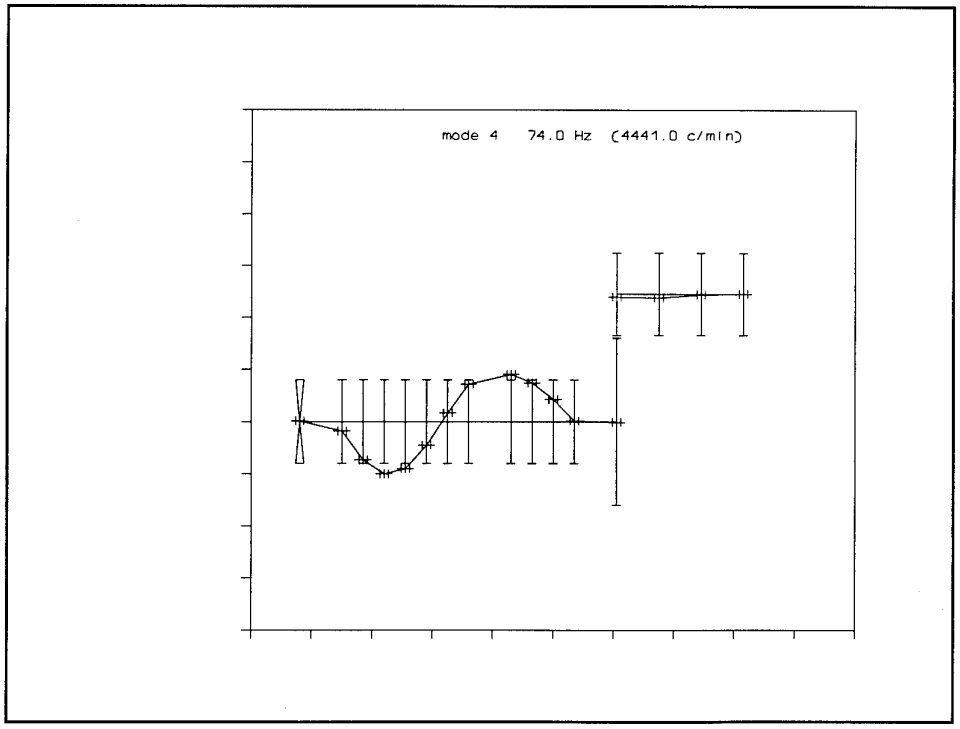

Figure 3.4 Mode 4

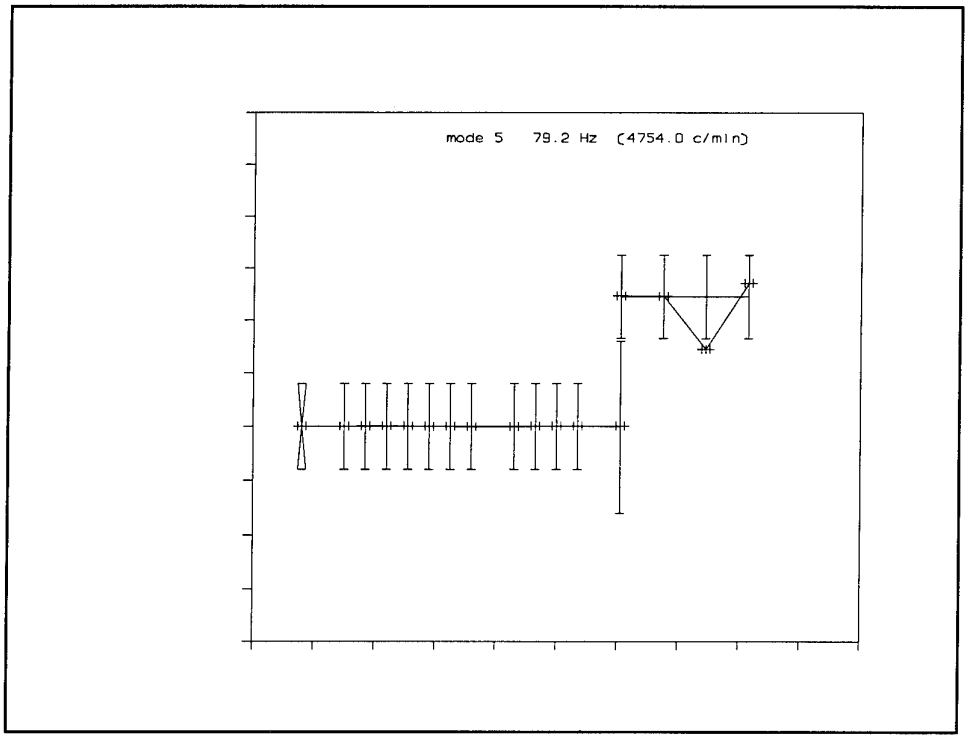

Figure 3.5 Mode 5

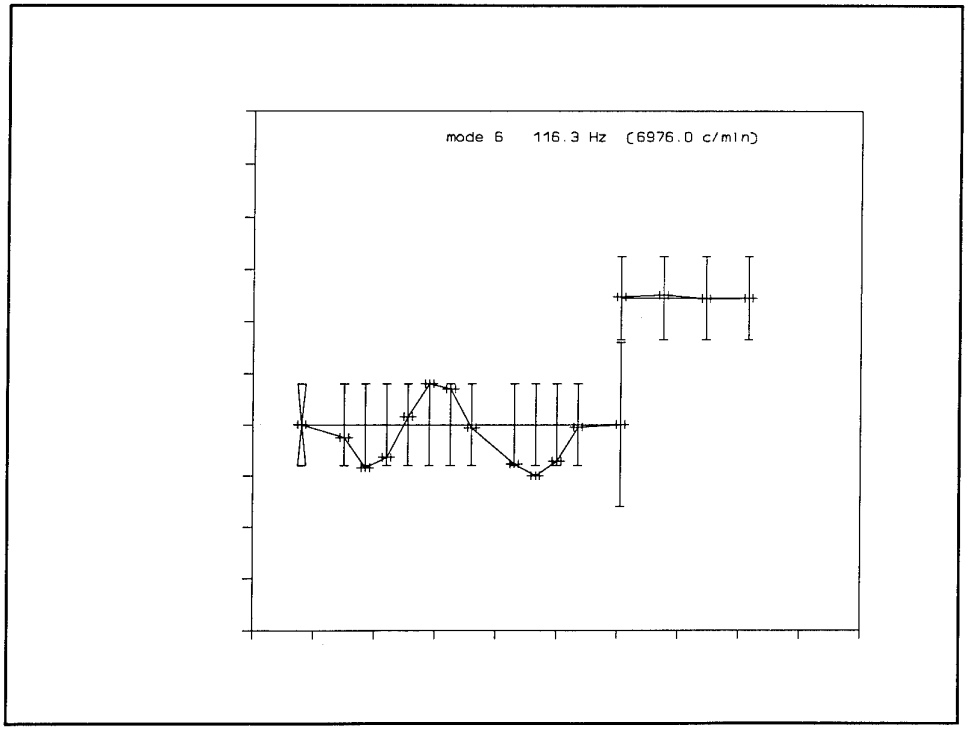

Figure 3.6 Mode 6

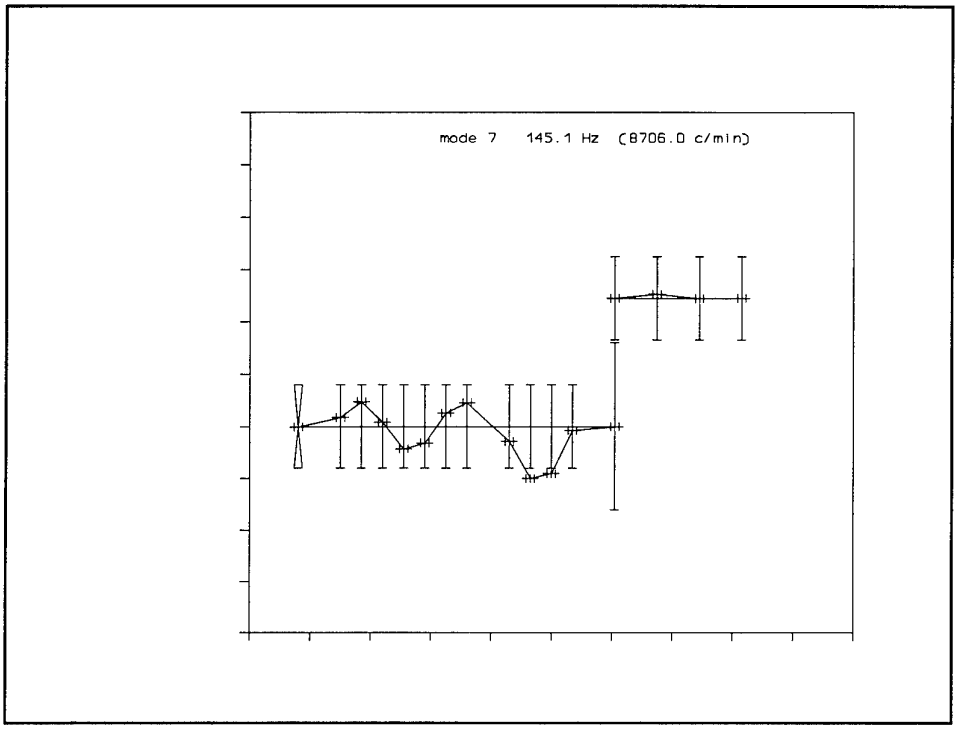

Figure 3.7 Mode 7

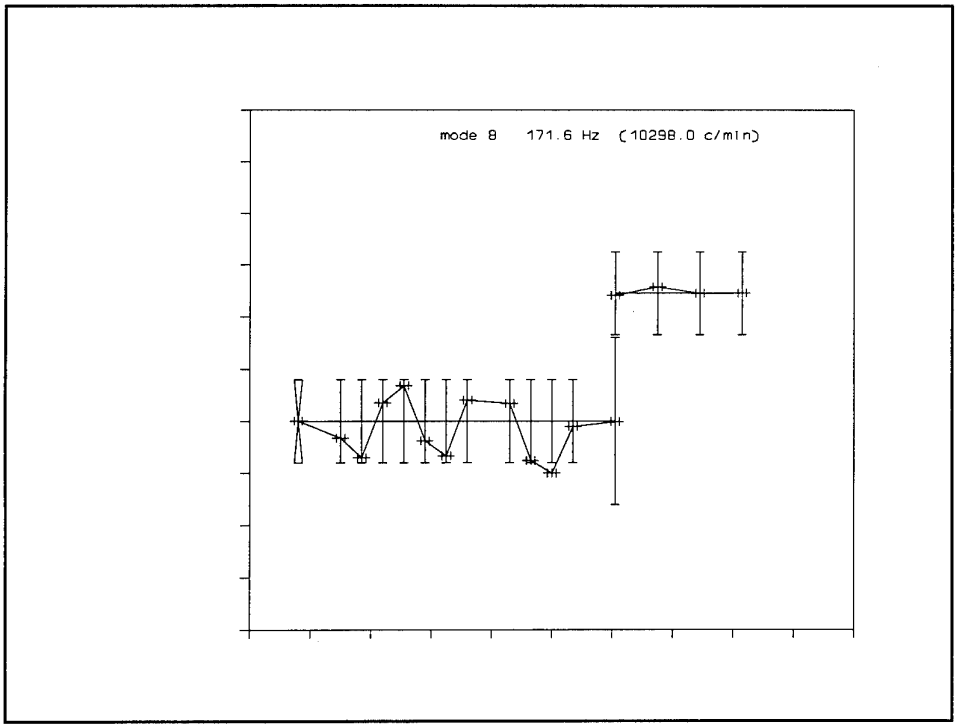

Figure 3.8 Mode 8

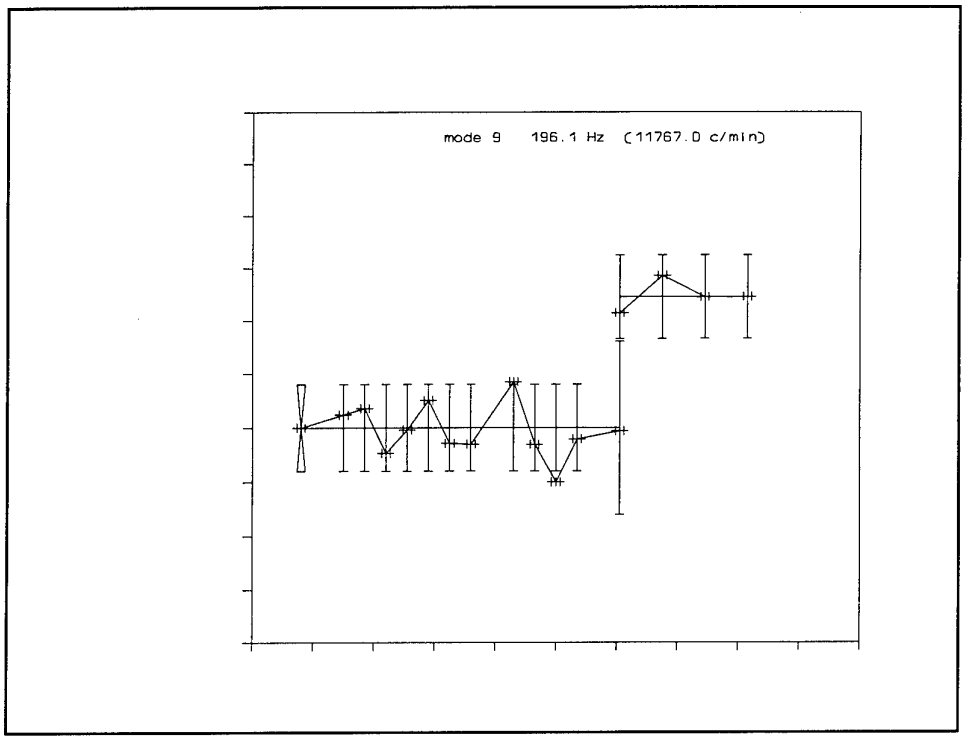

Figure 3.9 Mode 9

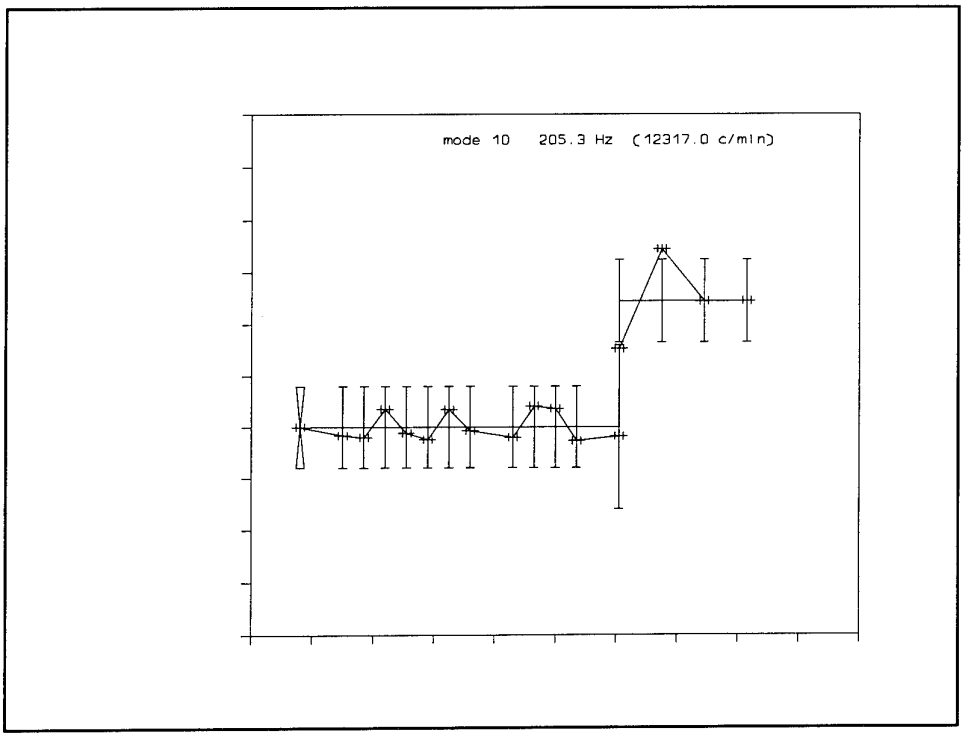

Figure 3.10 Mode 10

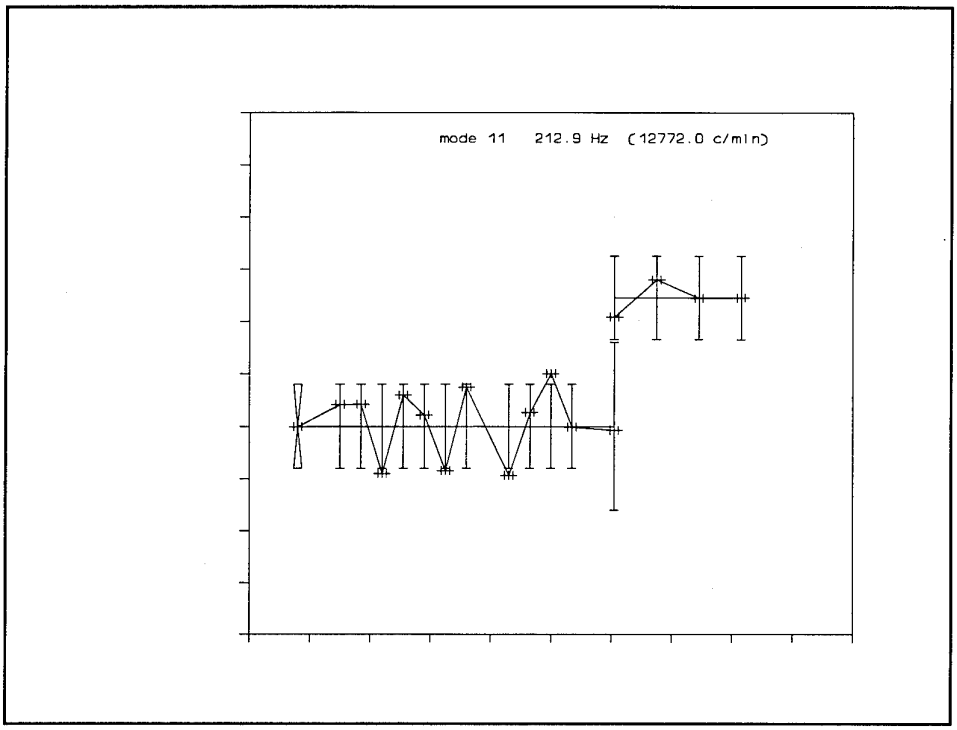

Figure 3.11 Mode 11

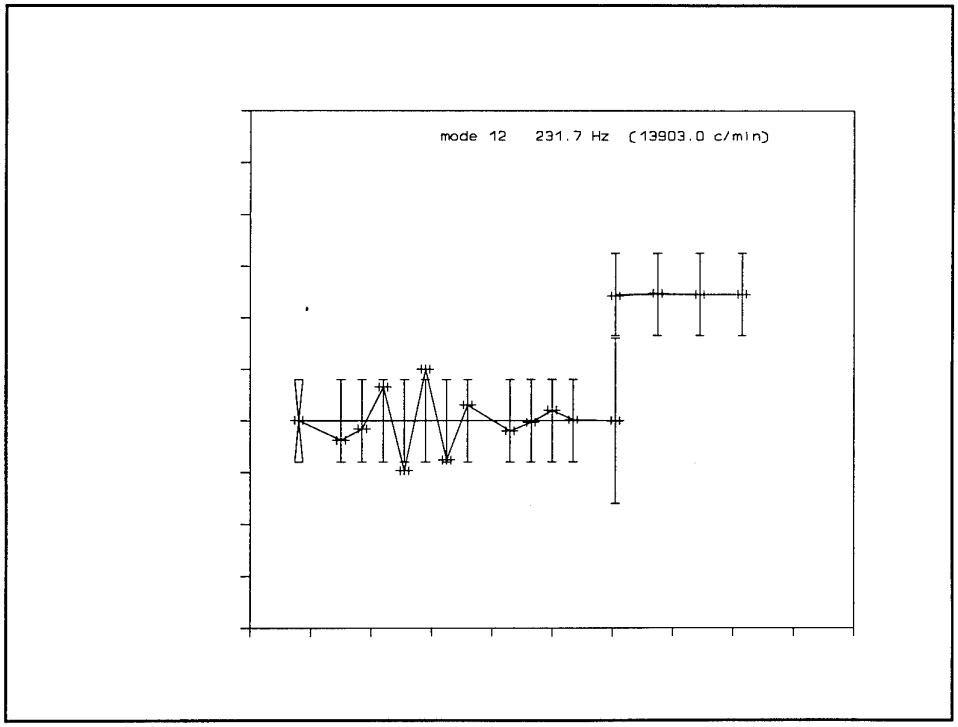

Figure 3.12 Mode 12

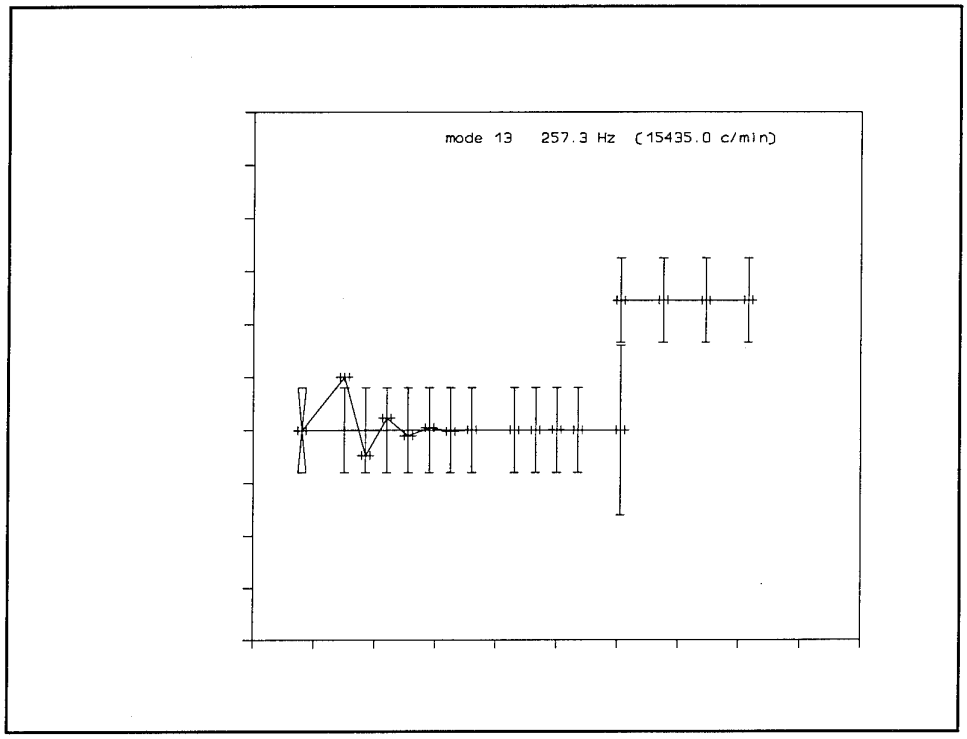

Figure 3.13 Mode 13

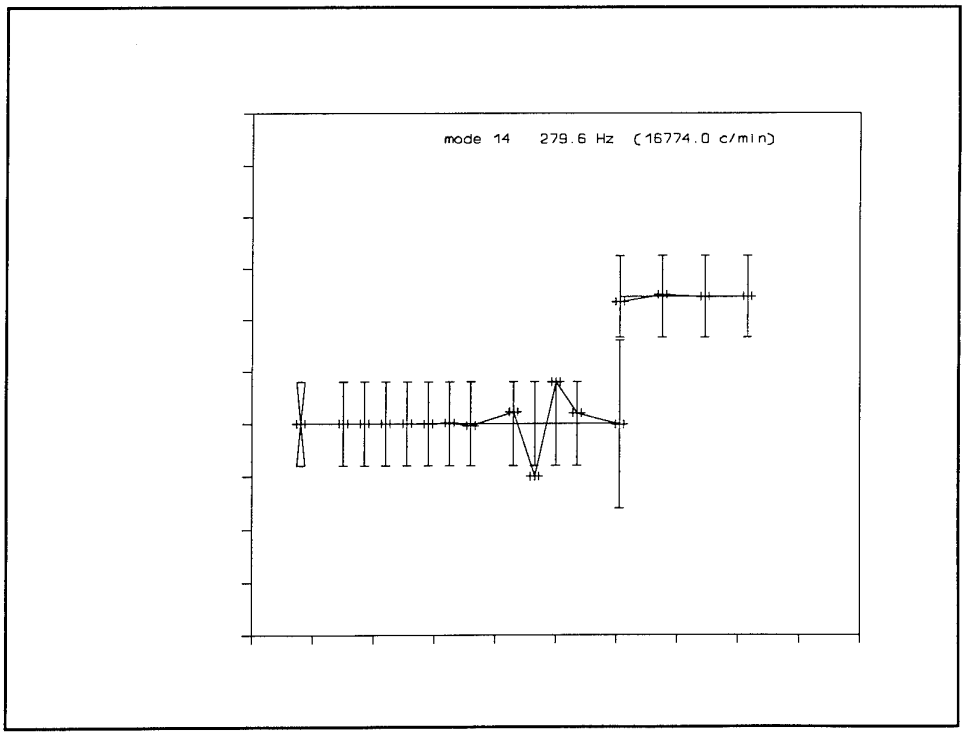

Figure 3.14 Mode 14

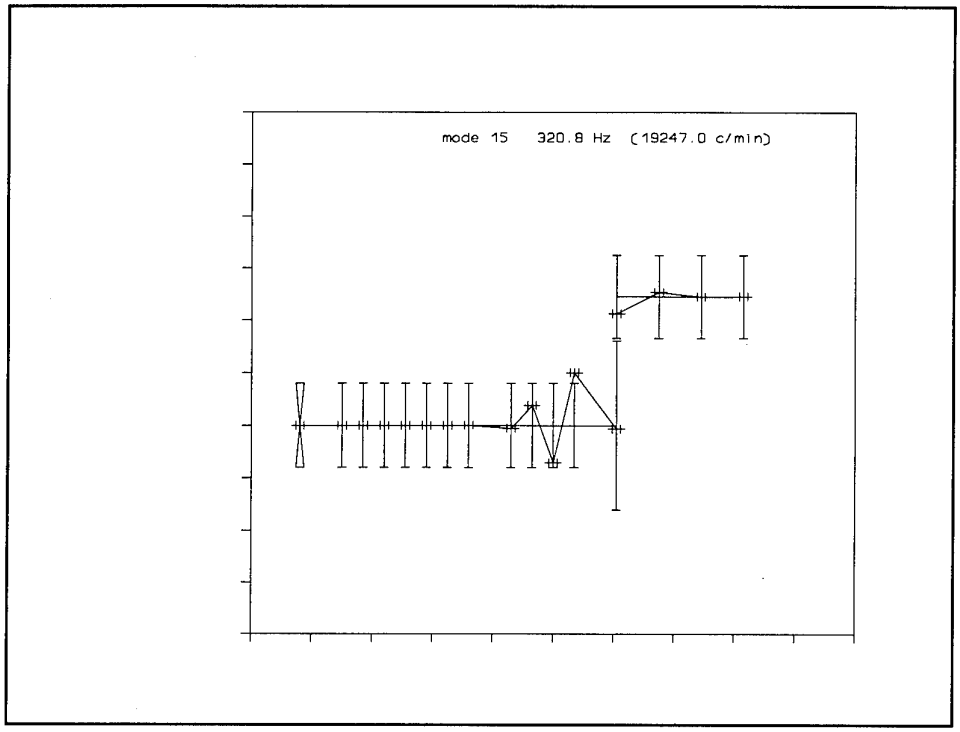

Figure 3.15 Mode 15

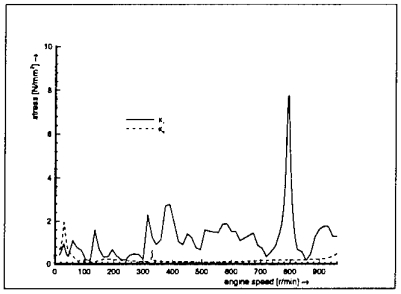

Figure 5.1 Vibratory stresses in the shaft of the electric motor (spring 1) and in the highest loaded part of the long propeller shaft (spring 6) as a function of the rotor speed

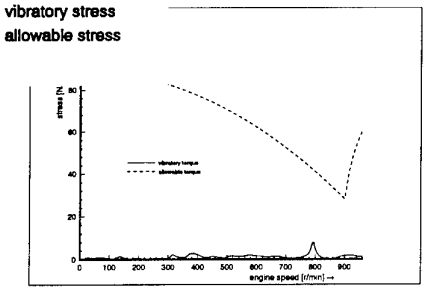

Figure 5.2 Vibratory stress in the shaft of the electric motor (spring 1) together with the allowable stress according to Lloyd's Register of Shipping

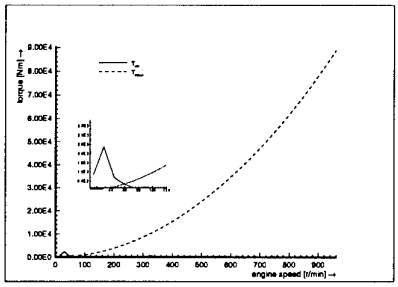

Figure 5.3 Vibratory torque and mean torque in the gear transmission

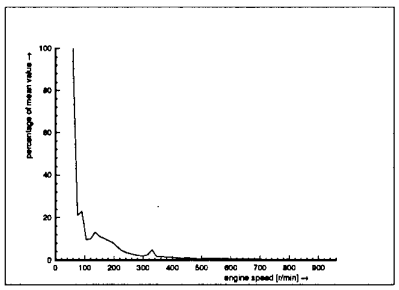

Figure 5.4 Vibratory torque in the gear transmission as a percentage of the mean torque

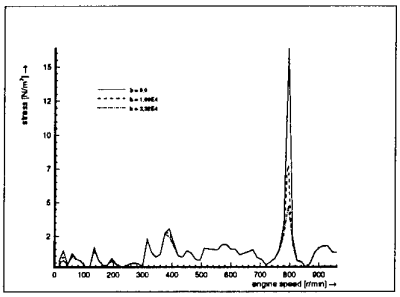

Figure 6.1 Vibratory stresses in the shaft of the electric motor (spring 1) for various values of the damping coefficient b_m (see **Note** at section 6.1)

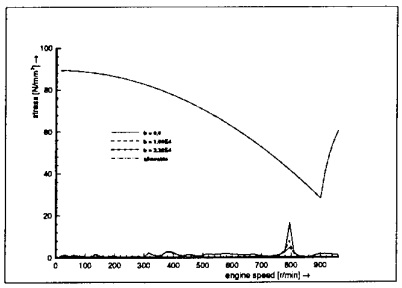

Figure 6.2 Vibratory stresses in the shaft of the electric motor for various values of the damping coefficient b_m together with the allowable stress according to Lloyd's Register of Shipping (see **Note** at section 6.1)

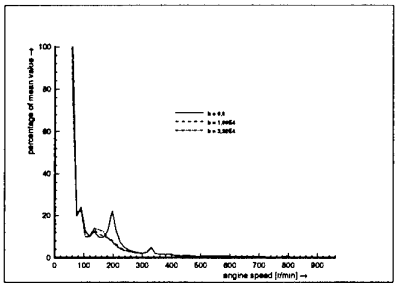

Figure 6.3 Vibratory torque in the gear transmission as a percentage of the mean torque for various values of the damping coefficient b_m (see **Note** at section 6.1)

Appendix A: Model of the asynchronous induction motor of the ATS

Model of the asynchronous induction motor of the ATS

For a torsional calculation of a propulsion installation with an asynchronous induction motor it is important to know the interaction between the mechanical system and the electric system. The dynamics of an induction motor is non-linear through the use of alternating current. It is complex to calculate the real input dynamics of the motor, because the interference of the higher harmonics of the motor voltage produces harmonic torque vibrations. Further, the controlled converter also produces higher harmonics. Because of the complexity of this problem, the higher harmonics have not been taken into account in the model of the electric motor. (In the torsional vibration analyses, these higher harmonics have been modelled as 'external forces' as described in section 2.2 of this report.)

In the following the torque/speed characteristics of the asynchronous induction motor is calculated for a steady-state situation. It turns out that the motor can be modelled by a mechanical viscous damper with a damper value of $1.66*10^5$ N.m.s/rad.
References used for this appendix are listed at the end of this appendix.

Steady-state model

In an induction motor a rotating field is produced in the air gap by the AC in the stator windings. This field interacts with the rotor windings to induce a voltage and hence a current into the rotor conductors. The torque is then produced by the interaction of the field and the rotor currents.
The speed of the rotation of the field is defined by the frequency ω_s of the AC supply and the number of poles p on the motor.
The difference between the synchronous speed and the actual speed ω_m of the rotor is expressed by the slip s:

$$s = \frac{\omega_s - (\omega_m\ p)}{\omega_s} \qquad [-] \qquad \textbf{(1)}$$

Figure 1 shows an equivalent circuit for one phase of an induction motor.

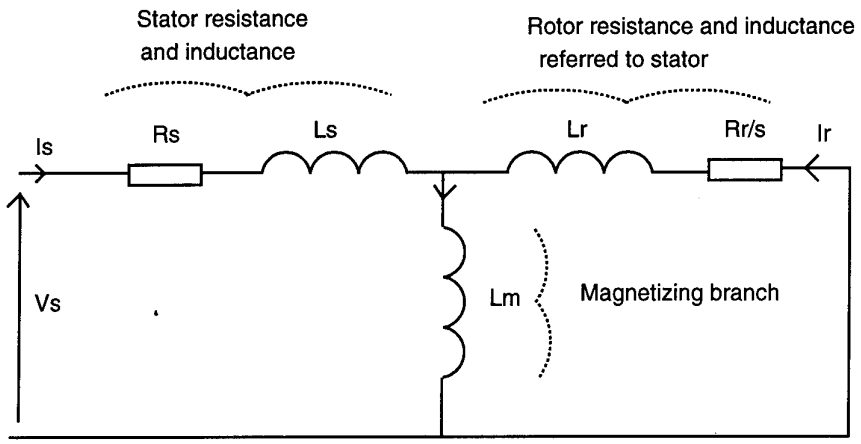

Figure 1 Equivalent circuit of one phase of an induction motor

In this figure:

I_s = stator current	[A]
I_r = rotor current	[A]
I_m - field current	[A]
V_s = effective phase voltage	[V]
R_s = stator resistance	[Ω]
L_s = stator stray inductance	[H]
L_m = magnetization inductance	[H]
L_r = rotor stray inductance	[H]
R_r = rotor resistance	[Ω]
s = slip	[-]

With the reactances denoted by X_s, X_m and X_r:

$X_s = \omega_s * L_s$	[V/A]
$X_m = \omega_s * L_m$	[V/A]
$X_r = \omega_s * L_r$	[V/A]

In the equivalent circuit of the induction motor the rotor circuit is translated to the stator circuit. The rotor system as seen by the stator can than be modelled as a resistance per phase of R_r/s. From the principle of conservation of energy the mechanical power is calculated. This power is:

$$P_m = T_m \omega_m \quad [W] \qquad (2)$$

The power transferred across the air gap into the rotor is:

$$P_{ag} = I_r^2 \frac{R_r}{s} \qquad [W] \qquad \textbf{(3)}$$

The power lost in the rotor resistance is:

$$P_r = I_r^2 R_r \qquad [W] \qquad \textbf{(4)}$$

The mechanical power is then:

$$P_m = P_{ag} - P_r = I_r^2 R_r \frac{(1 - s)}{s} = T_m \omega_m \qquad [W] \qquad \textbf{(5)}$$

With equation (1):

$$(1-s) = \frac{\omega_m p}{\omega_s} \qquad [-] \qquad \textbf{(6)}$$

it follows:

$$T_m = p \frac{I_r^2 R_r}{\omega_s s} \qquad [N.m] \qquad \textbf{(7)}$$

For an m-phase motor:

$$T_m = m\ p \frac{I_r^2 R_r}{\omega_s s} \qquad [N.m] \qquad \textbf{(8)}$$

From figure 1 the current I_r is calculated. The motor torque T_m is written as:

$$T_m = \frac{h\ s}{e + fs + gs^2} \qquad [N.m] \qquad \textbf{(9)}$$

With:

$$h = \frac{m\ p\ R_r\ V_s^2\ X_m^2}{\omega_s} \qquad [N.m.V^4.A^{-4}] \qquad \textbf{(10)}$$

and:

$e = a^2 + c^2$	$[V^4A^{-4}]$
$a = R_s * R_r$	$[V^2A^{-2}]$
$c = R_r * (X_s + X_m)$	$[V^2A^{-2}]$
$f = 2 * (dc - ab)$	$[V^4A^{-4}]$
$d = R_s * (X_r + X_m)$	$[V^2A^{-2}]$
$b = (X_s * X_m) + X_r (X_r + X_m)$	$[V^2A^{-2}]$
$g = b^2 + d^2$	$[V^4A^{-4}]$

Motor control

The majority of AC variable speed drives are based around the use of an inverter to provide a variable frequency supply to an induction motor. The maximum torque of an m-phase motor is found by:

$$\frac{dT_m}{ds} = \frac{h}{gs^2+fs+e} - \frac{hs(2gs+f)}{(gs^2+fs+e)^2} = 0 \qquad [N.m] \qquad \textbf{(11)}$$

The slip s is at maximum torque:

$$s_{Tmax} = R_s \frac{1}{\sqrt{R_s^2+(X_s+X_r)^2}} \qquad [-] \qquad \textbf{(12)}$$

The solution of s gives for T_{max} :

$$T_{max} = \frac{m\ p\ V_s^2}{2\omega_s \sqrt{R_s^2+(X_s+X_r)^2}+R_s} \qquad [N.m] \qquad \textbf{(13)}$$

The maximum torque is seen to be independent of the value of R_r. Ignoring the resistive term R_s, this equation can be written in terms of the supply frequency ω_s as:

$$T_{max} = \frac{m\ p\ V_s^2}{2\ (L_s+L_r)\ \omega_s^2} \qquad [N.m] \qquad \textbf{(14)}$$

In order to maintain T_{max} constant over a wide motor speed area the ratio V_s^2/ω_s^2 must be constant. This is controlled by the controller. In practice, the effect of the resistance R_s is to decrease the torque at lower speed. The controller compensates for this to increase the applied voltage at this lower speeds. In this case V_s/ω_s is no longer constant but varies. This is in fact a larger signal behaviour and has no effect on small rotation variations.
For small torque variations $dT/d\omega_m$ is of importance and is found by:

$$\frac{dT_m}{ds} = \frac{T_m}{s} - \frac{T_m^2}{s}\ \frac{(2gs+f)}{h\ s} \qquad [N.m] \qquad \textbf{(15)}$$

Written in real parameters and small s:

$$\frac{dT_m}{ds} = \frac{h}{e} = \frac{m\ p\ R_r\ V_s^2\ X_m^2}{\omega_s\{(R_s\ R_r)^2+R_r^2(X_s+X_m)^2\}} \qquad [N.m] \qquad \textbf{(16)}$$

For high frequencies $X_m >> R_s$:

$$\frac{dT_m}{ds} = \frac{m\ p\ R_r\ V_s^2\ X_m^2}{\omega_s\ R_r^2\ X_m^2} = \frac{m\ p\ V_s^2}{\omega_s\ R_r} \qquad [N.m] \qquad \textbf{(17)}$$

$$s = \frac{\omega_s - (\omega_m\ p)}{\omega_s} \quad \text{thus:} \quad \frac{ds}{d\omega_m} = \frac{-p}{\omega_s} \qquad [-] \qquad \textbf{(18)}$$

Then:

$$\frac{dT_m}{d\omega_m} = -\frac{dT_m}{ds} * \frac{ds}{d\omega_m} = -\frac{m\ p\ V_s^2}{\omega_s\ R_r} * \frac{p}{\omega_s} = -\frac{m\ p^2}{R_r}\ \frac{V_s^2}{\omega_s^2} = -R \qquad \textbf{(19)}$$

Thus the equivalent resistance is:

$$R = \frac{m\ p^2}{R_r}\ \frac{V_s^2}{\omega_s^2} \qquad [\Omega] \qquad \textbf{(20)}$$

Note
This result could also be found by using the equation of Kloss and small values of the slip s, as explained in [A.3].

Because the motor model delivers energy the equivalent resistance R is positive. So, for small torque fluctuations the motor behaves as a viscous damper.
Because V_s/ω_s is held constant by the controller the resistance R of the induction motor is also constant. In figure 2 this model and the torque/speed characteristics are given.

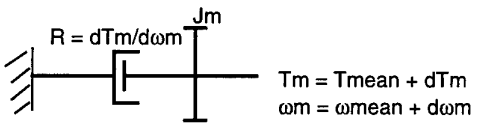

Simple vibration model of the controlled motor

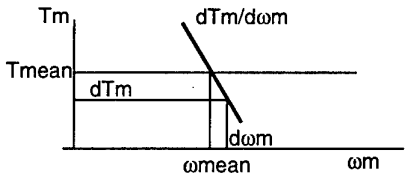

Controlled motor torque

Figure 2 Simple vibration model and controlled torque characteristics

The mean torque is held constant by the controller. The electric circuit of the motor is translated to the mechanical viscous damper R. The inertia J_m is the rotor of the motor.

Results for the electric motor of the ATS

The following preliminary data is used (final data used at the ATS is different):

nominal power of the ATS-motor	P_{norm}	=	7500	kW
effective phase voltage	$V_s = 3300/\sqrt{3}$	=	1905.26	V
stator resistance	R_s	=	0.0069758	Ω
stator stray inductance	L_s	=	$0.4817*10^{-3}$	H
magnetization inductance	L_m	=	$10.887*10^{-3}$	H
rotor stray inductance	L_r	=	$0.4343*10^{-3}$	H
rotor resistance	R_r	=	0.0073	Ω
slip frequency		=	0.36	Hz
slip at nominal power	$s_{norm} = 0.36/60.4$	=	$5.96*10^{-3}$	
nominal rotor speed	n_{norm}	=	906	r/min
nominal rotor frequency	f_{norm}	=	15.1	Hz
nominal AC frequency	$f_s = f_m * p$	=	60.4	Hz
nominal AC angular frequency	$\omega_s = 60.4 * 2\pi$	=	379.5	rad/s
pole pairs	p	=	4	
number of phases	m	=	3	
rotor inertia	J_m	=	540	$kg.m^2$

$$X_s = \omega_s * L_s \quad [V/A]$$
$$X_m = \omega_s * L_m \quad [V/A]$$
$$X_r = \omega_s * L_r \quad [V/A]$$

At $\omega_s = 60.4 * 2\pi = 379.5$ rad/s it follows:

$$X_s = 379.5 * 0.4817 * 10^{-3} = 0.1828 \text{ V/A}$$
$$X_m = 379.5 * 10.887 * 10^{-3} = 4.3132 \text{ V/A}$$
$$X_r = 379.5 * 0.4343 * 10^{-3} = 0.1648 \text{ V/A}$$

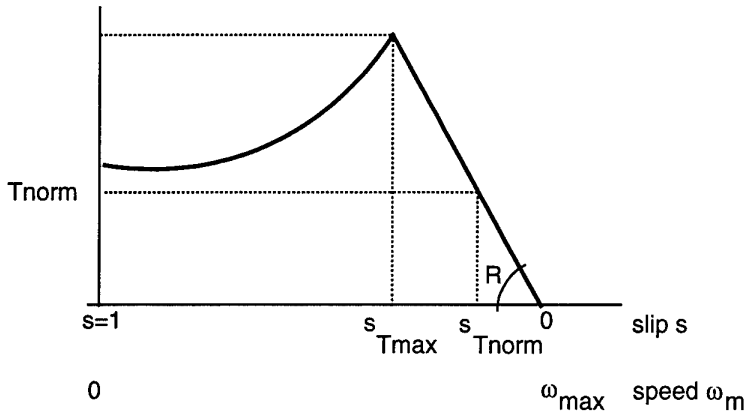

Figure 3 Torque/speed (torque/slip) characteristics of an induction motor

The characteristics of this motor as shown in figure 3 are as follows:

From equation (12):	s_{Tmax}	$= 0.021$
Specified above:	s_{norm}	$= 5.96*10^{-3}$
From equation (13):	T_{max}	$= 16.5*10^{4}$ N.m
From equation (9):	T_{norm}	$= 78.97*10^{3}$ N.m

This value for T_{norm} corresponds with the torque when calculated directly from the specified nominal power P_{norm} = 7500 kW and the specified nominal rotor speed = 906 r/min.

From equation (13):	T_{max}	$= 6550.21\ (V_s/\omega_s)^2$	[N.m]
From equation (19):	R	$= 6575.34\ (V_s/\omega_s)^2$	[N.m.s/rad]

At nominal load T_{norm} of the motor:

$$(V_s/\omega_s)^2 = 25.2\ V^2.s^2/rad^2$$

Then:

$T_{max} = 16.4*10^4$ N.m
R $= 1.66*10^5$ N.m.s/rad

This R is the required value for the mechanical viscous damper.

References at appendix A

[A.1] Slemon, G.R.
Electric Machines and Drives
ISBN 0-201-57885-9, University of Toronto, 1992

[A.2] Groot, D.J. de
Aandrijftechniek
Vakcode 13435, University of Twente, 1980

[A.3] Deleroi, W.
Elektrische machines 1B
Delft University of Technology, 1990

REPORT DOCUMENTATION PAGE

1. DEFENCE REPORT NUMBER (MOD-NL) TD 96 - 0102	2. RECIPIENT'S ACCESSION NUMBER	3. PERFORMING ORGANIZATION REPORT NUMBER 95-CMC-R0614
4. PROJECT/TASK/WORK UNIT NO. 42775649	5. CONTRACT NUMBER A94/KM/125	6. REPORT DATE December 31, 1995
7. NUMBER OF PAGES 51 (incl. appendix, excl. RDP and distribution list)	8. NUMBER OF REFERENCES 16	9. TYPE OF REPORT AND DATES COVERED Final Report

10. TITLE AND SUBTITLE

Torsional vibration analysis of a long propeller shaft system driven by an electric motor (Electric system)

11. AUTHOR(S)

H.S.T. Brockhoff, P.P.M. Lemmen

12. PERFORMING ORGANIZATION NAME(S) AND ADDRESS(ES)

Centre for Mechanical Engineering
Leeghwaterstraat 5
2628 CA DELFT, The Netherlands

13. SPONSORING/MONITORING AGENCY NAME(S) AND ADDRESSES(S)

Sponsor: Netherlands Ministry of Defence
Monitoring agency: TNO Defence Research, Schoemakerstraat 97, 2628 VK DELFT, The Netherlands

14. SUPPLEMENTARY NOTES

The Centre for Mechanical Engineering is part of TNO Building and Construction Research
The classification designation ONGERUBRICEERD is equivalent to UNCLASSIFIED.

15. ABSTRACT (MAXIMUM 200 WORDS, 1044 BYTES)

The report presents a torsional vibration analysis of a ship's propeller shaft system driven by an electric motor. The propeller shaft is unusual long: 43 meters. The results of the analysis are evaluated on basis of the specifications of Lloyd's Register of Shipping. Further, a comparison has been made with similar results using a diesel-direct propulsion system.

16. DESCRIPTORS	IDENTIFIERS
ship design propeller shaft vibration analysis	ship propulsion system electric propulsion system

17a. SECURITY CLASSIFICATION (OF REPORT)	17b. SECURITY CLASSIFICATION (OF PAGE)	17c. SECURITY CLASSIFICATION (OF ABSTRACT)
ONGERUBRICEERD	ONGERUBRICEERD	ONGERUBRICEERD

18. DISTRIBUTION/AVAILABILITY STATEMENT	17d. SECURITY CLASSIFICATION (OF TITLES)
Unlimited availability, requests shall be referred to sponsor	ONGERUBRICEERD

Distributielijst bij rapport 95-CMC-R0614
Instituut: TNO Bouw, CMC
Project A94/KM/125

DWOO	1
HWO-Centrale Organisatie	(B)
HWO-KM	1
HWO-KL	(B)
HWO-KLu	(B)
Projectbegeleider DMKM, afd. Platformsystemen, ir. I.P. Barendregt	4
Koninklijk Instituut voor de Marine ir. C.A.J. Tromp	2
Bureau TNO-DO	1
Bibliotheek KMA	3
Centrum voor Mechanische Constructies	9

(B) = Beperkt rapport